J. Plasma Phys. (2016), *vol.* 82, 635820305 © Cambridge University Press 2016
doi:10.1017/S0022377816000416

The Crab nebula energy origin and its high frequency radiation spectra

George Z. Machabeli[1,†], A. Rogava[1], N. Chkheidze[1], Z. Osmanov[2] and D. Shapakidze[1]

[1]Centre for Theoretical Astrophysics, ITP, Ilia State University, Tbilisi 0162, Georgia

[2]School of Physics, Free University of Tbilisi, 0183 Tbilisi, Georgia

(Received 17 January 2016; revised 6 April 2016; accepted 7 April 2016)

In the present work there is presented a model describing transfer of the Crab pulsar's spin-down energy into the powerful synchrotron emission of the nebula. The process of the energy transfer consists of several consecutive stages. The physical processes underlying the theoretical model provide us with the synchrotron emission spectrum, which fits well with the observed one.

1. Introduction

One of the major problems in astrophysics is finding the energy source for the emission of astrophysical objects. Along with such a powerful source as thermonuclear synthesis one should also study the possibility of rotational energy transfer of cosmic objects into their radiation. One of the obvious examples of such energy transformation is the emission from pulsars. Deutsch (1955) has considered a rotating sphere with the frozen-in dipolar magnetic field. It was shown that due to polarization of charges in the sphere the electromagnetic field is generated, with the component directed along the magnetic field outside the sphere (the analogue of Faraday's unipolar inductor). Based on this work, Goldreich and Julian constructed the basis for forming a self-consistent model for the pulsar magnetosphere (Goldreich & Julian 1969), which was developed and presented in the following paper (Sturrock 1971). The main idea of this work is that the total electrostatic potential falls in the region of magnetic poles, where the electric field extracts electrons from the star surface (forming the primary beam). It should be mentioned that extraction of positive ions is much more difficult (Ginzburg & Usov 1972). The extracted electrons propagate along the weakly curved magnetic field lines emitting gamma quanta, which in turn decay into electron–positron (e^-e^+) pairs: $\gamma + B \rightarrow \gamma' + B + e^- + e^+$ (Klepikov 1954; Erber 1966). We adhere to the view of Sturrock and Ruderman & Sutherland (Sturrock 1971; Ruderman & Sutherland 1975), considering that only electrons are ejected from the pulsar's surface, which is followed by birth of e^-e^+ pairs in the pulsar magnetosphere. We assume that the pulsar magnetosphere is filled with e^-e^+ plasma permeated with the primary electron beam, which appears to be the initial assumption not only for explaining the pulsar's emission properties but also the high-frequency radiation of the Crab nebula considered in the present paper.

† Email address for correspondence: g.machabeli@iliauni.edu.ge

https://doi.org/10.1017/S0022377816000416 Published online by Cambridge University Press

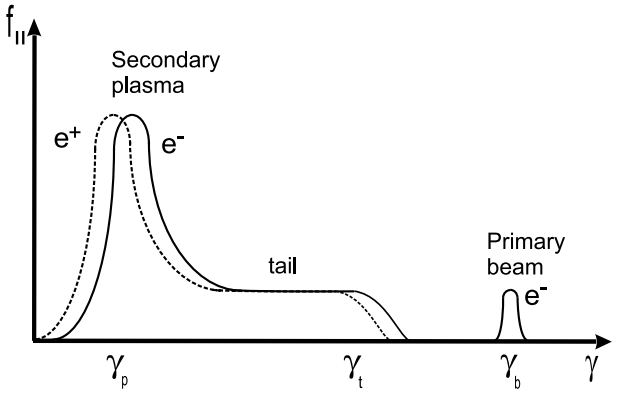


FIGURE 1. The distribution function of a one-dimensional plasma in the pulsar magnetosphere. Left corresponds to the secondary particles, right to the primary beam.

The only energy source of the observed radiation of the Crab nebula can be the pulsar located inside the nebula. The energy released due to spin slow-down of the pulsar PSR 0531+21 in a second equals

$$\frac{\mathrm{d}E}{\mathrm{d}t} = I\Omega\frac{\mathrm{d}\Omega}{\mathrm{d}t} = 5\times10^{38}\ \mathrm{erg\ s^{-1}}, \tag{1.1}$$

where $\Omega = 200\ \mathrm{s^{-1}}$ is the frequency of the pulsar rotation and $I = 10^{45}\ \mathrm{g\ cm^2}$ is the moment of inertia of the neutron star. This energy is enough to explain the total luminosity of the nebula $\mathrm{d}W/\mathrm{d}t = 5\times10^{38}\ \mathrm{erg\ s^{-1}}$. Note that the power of the pulsed emission of the pulsar itself is only about 1 % of the total radiation power. In order to emit photons with the energy up to 100 MeV, the electrons should possess the energy of the order of 1 PeV. Tademaru (1973) and Cocke (1975) have noticed that the energy of the particles injected by the pulsar into the nebula cannot be exceeding TeV energies, as due to energy losses through the radiation processes.

Let us consider the possibility of energy supply of a nebula by kinetic energy of particles. The mechanism of particle production and acceleration in pulsar magnetospheres is well defined through the series of works (Klepikov 1954; Deutsch 1955; Erber 1966; Goldreich & Julian 1969; Sturrock 1971; Tademaru 1973; Ruderman & Sutherland 1975; Michel 1982) etc. The distribution function of magnetospheric plasma particles consists of three types of particles: the bulk of the plasma with the particle concentration at the star surface $n_p \approx 10^{20-21}\ \mathrm{cm^{-3}}$ and the Lorentz factor $\gamma_p \approx 10^2$ when the magnetic field is dipolar and for the quadrupole magnetic field $\gamma_p \approx (3\text{–}10)$ (Machabeli & Usov 1989), the long extended in one direction tail of the distribution function with $\gamma_t \approx (10^3\text{–}10^5)$, $n_t \approx (10^{16}\text{–}10^{17})\ \mathrm{cm^{-3}}$, and the most energetic primary beam with $\gamma_b \approx (10^6\text{–}10^7)$, $n_b \approx (10^{11}\text{–}10^{12})\ \mathrm{cm^{-3}}$ (Tademaru 1973; Arons 1981) (see figure 1). In this case the maximum energy density of the electron flux is $mc^2 n_{GJ}\gamma_b$, where $n_{GJ} = 7\times10^{-2}B_s\ P^{-1}$ is the number density of particles extracted from the pulsar surface by action of the electric field, generated due to rotation of the magnetized star (here B_s is the magnetic field at the star's surface and P is the pulsar rotation period) (Goldreich & Julian 1969). The density of the primary beam near the light cylinder $n_{GJ} \sim 10^6\ \mathrm{cm^{-3}}$. Now if we multiply the flux energy density of the primary particles by the volume of the

https://doi.org/10.1017/S0022377816000416 Published online by Cambridge University Press

light cylinder and divide by time R_{Lc}/c, which is necessary for the transfer of the energy on the light-cylinder length scales, we will find that the power provided by the particle flux is equal to

$$mc^3 n_{GJ}\gamma_b R_{Lc}^2 \sim 10^{33}\ \text{erg s}^{-1}. \tag{1.2}$$

It is obvious that the obtained quantity is not big enough to explain the observed luminosity, which inevitably shows the necessity of the additional acceleration of the particles.

In a superstrong pulsar magnetic field the flux of the magnetospheric e^-e^+ plasma is directed along the open magnetic field lines, which, along with magnetospheric plasma, mutually rotates with the star. In § 2 we consider in detail a problem of the motion of a relativistic particle along a rotating rigid string (Machabeli & Rogava 1994). The paper considering this problem provided us with a theoretical framework that was later used to consider the problem of pulsar rotational energy pumping into the electrostatic waves of magnetospheric plasma (Machabeli *et al.* 2005; Mahajan *et al.* 2013; Machabeli *et al.* 2015). Section 3 is devoted to considering this problem, where we show that the pulsar rotational energy is pumped into the Langmuir perturbations mainly in the long-wavelength region, where the phase velocity of the wave exceeds the speed of light $v_{ph} = \omega/k > c$. As particles with such speed do not exist, the waves propagate without damping. Consequently, the so-called 'condensate' of electrostatic perturbations is produced, which is transferred into the nebula. This particular process is considered in § 4. Unlike the pulsar magnetosphere, in the nebula region there are also ions; consequently, there are low-frequency electrostatic oscillations, in particular ion sound. This ensures the collapse process of the Langmuir waves that is described in § 5. Collapse itself causes particle acceleration through the Landau damping process that can result in particle acceleration up to very high Lorentz factors. Such ultrarelativistic particles can provide generation of very high frequency emission through the synchrotron radiation process, which is considered in § 6. In § 7 we obtain the spectrum of the synchrotron emission of the nebula and finally in § 8 we make conclusions.

2. Dynamics of a particle moving along a straight rigid rotating string

The problem of a particle motion along a straight rotating string implies investigating the following equation:

$$\frac{\mathrm{d}\boldsymbol{P}}{\mathrm{d}t} = 0. \tag{2.1}$$

Here the change of the momentum $\mathrm{d}\boldsymbol{P}$ in the time interval $\mathrm{d}t$ consists of two parts; one is the change of momentum in the given point of space and the other is the difference of momenta that the particle has in two different space points separated from each other with a space interval $\mathrm{d}\boldsymbol{r}$, the distance that the particle covers in time $\mathrm{d}t$ (substantial derivative). Now let us consider figure 2, which shows the two different positions of the particle moving along the rotating straight string, the initial position and the position after time $\mathrm{d}t$, i.e. the time during which the string rotated by the angle $\Omega\,\mathrm{d}t$ around the spin axis; here Ω is the rotation frequency of the string. One can introduce unit vectors along and across the string $\boldsymbol{h} = \boldsymbol{P}_\parallel/P_\parallel$ and $\boldsymbol{n} = \boldsymbol{P}_\perp/P_\perp$. For the relativistic particle $P_\parallel = m\upsilon_\parallel\gamma$, $P_\perp = m\upsilon_\perp\gamma$, $\upsilon_\perp = \Omega r$ and $\gamma = [1-(\upsilon_\parallel^2 + \Omega^2 r^2)/c^2]^{-1/2}$. The particle momentum can be written in the following form:

$$\boldsymbol{P} = \boldsymbol{h}P_\parallel + \boldsymbol{n}P_\perp. \tag{2.2}$$

https://doi.org/10.1017/S0022377816000416 Published online by Cambridge University Press

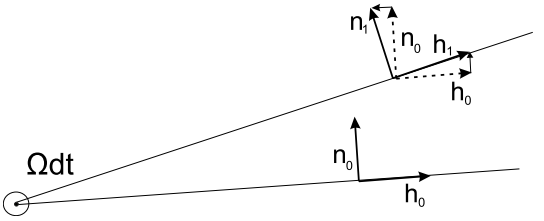


FIGURE 2. Particle motion along a rigid rotating string. $\boldsymbol{h}$ and $\boldsymbol{n}$ are the unit vectors along and across the string.

As we are interested in particle motion along the string, let us multiply (2.1) by $\boldsymbol{h}$. Taking into account (2.2) and the following expressions (see figure 2):

$$\boldsymbol{h}\cdot\boldsymbol{n}=0,\quad \boldsymbol{h}\cdot\frac{\mathrm{d}\boldsymbol{h}}{\mathrm{d}t}=0,\quad \boldsymbol{h}\cdot\frac{\mathrm{d}\boldsymbol{n}}{\mathrm{d}t}=-\Omega, \tag{2.3a–c}$$

one can write

$$\boldsymbol{h}\cdot\frac{\mathrm{d}\boldsymbol{P}}{\mathrm{d}t}=\frac{\partial P_{\parallel}}{\partial t}-\Omega P_{\perp}=0. \tag{2.4}$$

The second term of this equation corresponds to the second term of the substantial derivative. Taking into account the relativistic character of the particle motion $\Omega P_{\perp}=m\Omega^2 r\gamma$, $\partial P_{\parallel}/\partial t=m\gamma\,\partial\upsilon_{\parallel}/\partial t+m\upsilon_{\parallel}\partial\gamma/\partial t$, $\mathrm{d}r/\mathrm{d}t=\upsilon_{\parallel}$ and $\partial\gamma/\partial t=\gamma^3/c^2\upsilon_{\parallel}(\partial\upsilon_{\parallel}/\partial t+\Omega^2 r)$, one can finally rewrite (2.1) as follows:

$$\frac{\mathrm{d}^2 r}{\mathrm{d}t^2}=\frac{\Omega^2 r}{1-\Omega^2 r^2}\left[1-\Omega^2 r^2-2\left(\frac{\mathrm{d}r}{\mathrm{d}t}\right)^2\right]. \tag{2.5}$$

This equation describes 'Huygens's pendulum', having the exact analytical solution that is expressed by Jacobi functions, which, for ultrarelativistic particles, can be reduced to the form

$$\upsilon\equiv\frac{\mathrm{d}r}{\mathrm{d}t}\approx c\cos(\Omega t+\Phi), \tag{2.6}$$

where Φ is the initial phase.

From the analysis of (2.5), it becomes evident that on the light-cylinder surface the radial velocity should vanish. In particular, by applying the method developed by Machabeli & Rogava (1994), it has been shown that υ close to the mentioned zone behaves as follows (Osmanov 2011):

$$\upsilon\approx c\left(1-\frac{\Omega^2 r^2}{c^2}\right)^{1/2}, \tag{2.7}$$

leading to the radial acceleration $-2\Omega c$ (see (2.5)). This means that the radial velocity must change its sign. On the other hand, the time derivative of the radial component of momentum, $\dot{P}_r=m\gamma\Omega^2 r$, is always positive, never changing its sign. This is not a contradiction because in the framework of the above analysis it has been assumed that rigid rotation is maintained up to the light-cylinder area, which is not correct. It should be mentioned that the present problem was solved for idealized conditions, including not taking into account the conservation of angular momentum for the closed system

https://doi.org/10.1017/S0022377816000416 Published online by Cambridge University Press

and also the influence of the relativistic growth of particle weight on the frequency of the neutron star's rotation in case of open systems. In the paper by Machabeli *et al.* (1996), it was shown that up to a certain distance near the light cylinder one can assume that the system is closed and the Lorentz factor is constant. At higher distances, closer to the light cylinder, the picture changes dramatically, as the particle is so much accelerated that the star rotation is stopped. In other words, if the virtual string stays strictly straight the pulsar rotation energy is entirely transferred into the particle energy (see appendix A). Of course this virtual experiment is not realistic; on the other hand, it well demonstrates the potential possibilities of the mentioned mechanism.

For constraining a more realistic model, one needs to investigate the process of twisting of the magnetic field lines in the opposite direction from rotation (Michel 1969; Bogovalov 2001; Rogava *et al.* 2003; Osmanov *et al.* 2008, 2009). Therefore, the above equations are valid inside the light-cylinder zone and the developed method cannot be extended in the region outside the light cylinder. We will return to this issue later. In the next section we consider the possibility of a neutron star's rotation energy pumping into the energy of eigen electrostatic waves of magnetospheric plasma.

3. Parametric mechanism of pumping of rotation energy into that of Langmuir waves

In this section we consider the flux of the magnetospheric particles moving along the field lines of a very strong magnetic field. For this purpose, we expand the physical quantities around unperturbed values keeping up to linear terms

$$\Psi \approx \Psi^0 + \Psi^1, \tag{3.1}$$

where $\Psi = \{n, \boldsymbol{v}, \boldsymbol{p}, \boldsymbol{E}, \boldsymbol{B}\}$.

One can show that the centrifugal force close to the light cylinder reduces to $m\gamma\Omega^2 r\upsilon/c$ (Thorne *et al.* 1986; Machabeli *et al.* 2005). In order to derive a perturbed term of the centrifugal force, we expand the Lorentz factor by means of the dimensionless momentum, $\boldsymbol{p} \equiv \boldsymbol{p}/mc$,

$$\gamma \approx (1 + (\boldsymbol{p}^0 + \boldsymbol{p}^1)^2)^{1/2} \approx \left(1 + \left(\boldsymbol{p}^{\boldsymbol{0}}\right)^2\right)^{1/2} \left(1 + \frac{2\boldsymbol{p}^0\boldsymbol{p}^1}{1 + \left(1 + \left(\boldsymbol{p}^{\boldsymbol{0}}\right)^2\right)^{1/2}}\right)^{1/2} \approx p^0 + p^1, \tag{3.2}$$

leading to the following expression of the centrifugal force:

$$\boldsymbol{F} = m\Omega^2 p^1 \frac{\upsilon^0}{c}\boldsymbol{r}, \tag{3.3}$$

where we have taken into account the relations $p^0 \gg 1 \gg 2p^1/p^0$ and υ^0 is given by (2.6). This can be straightforwardly derived by applying the frozen-in condition of plasmas, $\boldsymbol{E^0} + \upsilon^{\boldsymbol{0}} \times \boldsymbol{B^0} = 0$. The corresponding equation can be obtained by replacing $\mathrm{d}/\mathrm{d}t$ by the quasistationary derivative, maintaining the first-order terms. This equation must be combined with the continuity and the Poisson equations, respectively,

$$\left.\begin{aligned} \frac{\partial p_\beta}{\partial t} + \upsilon_\beta \frac{\partial p_\beta}{\partial r} &= F_\beta + e_\beta E, \\ \frac{\partial n_\beta}{\partial t} + \frac{\partial (n_\beta^0 \upsilon_\beta)}{\partial r} + \frac{\partial (n_\beta \upsilon_\beta^0)}{\partial r} &= 0, \\ \frac{\partial E}{\partial r} &= 4\pi \sum_\beta e_\beta n_\beta, \end{aligned}\right\} \tag{3.4}$$

https://doi.org/10.1017/S0022377816000416 Published online by Cambridge University Press

where β denotes the species of plasma particles. The above set of equations does not contain the perturbed magnetic field because we study generation of the electrostatic field along the magnetic field lines.

For studying the excitation of Langmuir waves, we consider two plasma components with different Lorentz factors. The relatively low-energy plasma component we will denote by the subscript 'p' and the high-energy beam component with the subscript 'b'.

From the aforementioned system of equations, it is clear that these two components are mathematically linked by the mutual electrostatic field. After Fourier transformation and by applying a method developed in a series of papers (Machabeli *et al.* 2005; Mahajan *et al.* 2013; Osmanov *et al.* 2014, 2015), equations (3.4) reduce to a single equation

$$\left(\omega^2-\frac{\omega_p^2}{\gamma_p^3}\right)N_p(\omega)=\frac{\omega_b^2}{\gamma_b}\sum_{l,s}\mathrm{I}_l(a)\mathrm{I}_s(a) \times\left[\frac{\omega-(s-l)\Omega}{\omega-s\Omega}\right]^2 \mathrm{e}^{\mathrm{i}(l\phi_p-s\phi_b)}N_p(\omega+(l-s)\Omega), \tag{3.5}$$

where $N_p(\omega)=n_p\mathrm{e}^{\mathrm{i}a\sin(\Omega t+\phi_p)}$, $a=kc/\Omega$, I_s is the Bessel function of the first kind and ϕ_p and ϕ_b are the phases of the plasma and beam components, respectively.

By averaging (3.5) with the phases, it is clear that on the right-hand side of the equation the non-zero terms come from those with $\phi_p=\phi_b$ when $l=s$ (the equal phases means that initially the particles are at equal distances from the pulsar). As a result, the dispersion relation may be written as

$$\left(\omega^2-\frac{\omega_p^2}{\gamma_p^3}\right)=\frac{\omega_b^2}{\gamma_b}\sum_s\mathrm{I}_s^2(a)\frac{\omega^2}{(\omega-s\Omega)^2}. \tag{3.6}$$

By expressing $\omega=\omega_0+\Delta$, where $\omega_0^2=2\omega_p^2/\gamma_p^3$, $\omega_0=s\Omega$, one can see that (3.6) contains two resonances, which must be satisfied simultaneously. After substituting the aforementioned expansion of ω into (3.6), we will obtain a cubic equation for Δ, having the following solution:

$$\mathrm{Im}\,(\Delta)=\frac{\sqrt{3}}{2}\left(\frac{\omega_0{\omega_b}^2}{2}\right)^{1/3}\mathrm{I}_s(a)^{2/3}, \tag{3.7}$$

where $\omega_b^2=4\pi n_b e^2/m$, $s=\omega_0/\Omega$ and $\mathrm{Im}\,(\Delta)$ is the instability increment describing the efficiency of excitation of the centrifugally induced Langmuir waves. The growth rate is very sensitive to a value of the Bessel function. One should note that for large arguments, $a\gg 1$, the Bessel function is maximum for equal values of the index and argument, $a=s$ (Abramowitz & Stegun 1965). Therefore, in the parametric interaction of particles and waves, the leading terms come from the higher harmonics, $s\gg 1$.

It is significant to know the fraction of energy of the Langmuir waves that is consumed in the plasma magnetospheres. An efficient mechanism of energy dissipation of waves is the Landau damping, which takes place when the phase velocity does not exceed the flow velocity of plasmas. For this, one needs to know the critical wave number, k_c, when the dispersion curve intersects the $\omega=kc$ line.

https://doi.org/10.1017/S0022377816000416 Published online by Cambridge University Press

The electrostatic waves are described by the following equation:

$$1 - \sum \omega_p^2 \int \frac{f(p)\,\mathrm{d}p}{(\omega - k\upsilon)^2 \gamma^3} = 0, \tag{3.8}$$

where summation is performed with species of particles – electrons and positrons, $\omega_p^2 = 8\pi n_p e^2/m$ and $f(p)$ is the normalized plasma distribution function.

The above equation can be straightforwardly solved in two extreme limits: $\omega \gg k\upsilon$ and $\omega \approx kc$. In the first case when the phase velocity exceeds that speed of light, the dispersion relation may be written as

$$\omega^2 = \frac{\omega_p^2}{\gamma^3} + 3k^2c^2. \tag{3.9}$$

Considering the second limit, we substitute $\omega \approx kc$ and $\upsilon = c(1 - 1/\gamma^2)^{1/2}$ into $(\omega - k\upsilon)^2$. Then, if we expand the square root with respect to the small parameter, $1/\gamma^2$, from the aforementioned equation we will obtain an expression of the critical wave vector

$$\frac{\omega^2}{c^2} = k_c^2 = 2\gamma \frac{\omega_p^2}{c^2}, \tag{3.10}$$

when the spectrum is the following (Lominadze *et al.* 1979):

$$\omega = kc\left(1 - \alpha \frac{k - k_c}{k}\right). \tag{3.11}$$

From (3.5), it is clear that $\omega_0 < k_c c$ and the condition $\omega_0 = kc$ is satisfied when $k < k_c$. Consequently, the increment reaches its maximum value for the superluminal area of the phase velocity $\omega_0/k < \omega_0/k_c \approx c$. There are no such particles in the plasma magnetospheres; therefore, the Langmuir waves might interact with particles of the electron–positron plasma only by means of the nonlinear effects. It is worth noting that due to the parametric instability the pulsar's rotation energy is directly pumped into the electrostatic waves. One can straightforwardly estimate from (2.5) the power of the parametric mechanism

$$W_t = \frac{\Omega^2 r c^3}{1 - \dfrac{\Omega^2 r^2}{c^2}} \approx \frac{10^{36}}{1 - \dfrac{\Omega^2 r^2}{c^2}}\ \mathrm{erg\ s^{-1}}. \tag{3.12}$$

From this equation, it is evident that close to the light-cylinder surface $\Omega r/c \lesssim 1$ the power asymptotically increases very rapidly and under the condition of rigid rotation tends to infinity. Although in real astrophysical scenarios such a condition cannot be maintained for the whole course of motion and under different circumstances, the rigid rotation will inevitably be violated and, as we know, the aforementioned power may reach the typical value for the Crab pulsar 5×10^{38} erg s^{-1}. According to a series of works, such a limit is a direct result of reconstruction of the magnetic field from a dipolar structure to the poloidal configuration (Michel 1969; Osmanov *et al.* 2008, 2009). In these works it has been shown that by means of the parametric instability the poloidal magnetic field is created and the process is terminated when the dynamics becomes force-free. On the other hand, as was found by Rogava *et al.* (2003), in the force regime of dynamics the shape of trajectories in the local frame of reference

https://doi.org/10.1017/S0022377816000416 Published online by Cambridge University Press

must be described by the Archimedes spiral. Unlike this work, where the problem has been studied in a single-particle approach, Bogovalov (2001) has considered the problem by introducing the magnetic field and obtained a similar result. Therefore, outside the light-cylinder area the shape of field lines will inevitably reconstruct to the Archimedes spiral.

Instead of the field lines, one also can consider the magnetic flux as one does when considering general laws of electrodynamics, for instance, studying Gauss' theorem for magnetic fields. By analogy with the well-known problem of differential rotation of a fluid, when constituent particles do not experience forces and the flow is force-free, one can examine the magnetic field having the similar morphology providing the force-free dynamics (Machabeli *et al.* 2000).

In Osmanov *et al.* (2009), we have shown that the Goldreich–Julian current density, $\mathrm{J}_{GJ} = en_{GJ}c$, might create the toroidal magnetic field of the order of $4\pi \mathrm{J}_{GJ}R_{in}$, where $n_{GJ} = \Omega B/2\pi ec$ is the Goldreich–Julian particle number density and $R_{in} \approx B/(\partial B/\partial R)$ is the length scale of the inhomogeneity of the magnetic field. By assuming the dipolar magnetic field, one can show that an expression of the toroidal component is given by $2B/3$, which is not enough and, therefore, the aforementioned current cannot provide the required additional magnetic field. On the other hand, one can check that the Goldreich–Julian current exceeds the curvature drift current. This in turn means that the latter cannot be the source of B_r, although, as has been shown in Osmanov *et al.* (2009), it can be a trigger mechanism for excitation of the current, $\mathrm{J}_1 = e(n_b^0\upsilon_b^1 + n_b^1\upsilon_b^0)$ (superscripts 0 and 1 denote the unperturbed and perturbed quantities, respectively), which, by means of the parametric instability, will inevitably lead to the toroidal component of the magnetic field. As a result of the centrifugally induced instability, the magnetic field will be twisted. On the other hand, this process lasts until the particles experience the 'reaction' force, which, in turn, decreases more and more as the shape of the field lines locally tends to the configuration of the Archimedes spiral, when the instability completely vanishes terminating the subsequent twisting of the field lines. Generally speaking, the generation of the toroidal component of the magnetic field requires a certain power (Osmanov *et al.* 2009)

$$L_m \approx \frac{B_r^2}{4\pi T}\Delta V, \tag{3.13}$$

where $T \approx 1/|\mathrm{Im}\,(\Delta)|$ is the instability time scale, $\Delta V \approx R_{lc}^3\epsilon$ is the volume close to the light-cylinder area where the process takes place, $R_{lc} = c/\Omega$ is the light-cylinder radius and $\epsilon \sim 0.1$. For the typical parameters of the Crab pulsar the magnetic luminosity is only 5×10^{-5} % of the total bolometric luminosity. Therefore, this mechanism is feasible and will inevitably be developed in the magnetosphere close to the light-cylinder zone.

4. Pulsar rotation energy transfer by the Langmuir oscillations into the nebula

Previously, we have shown that the parametric generation of Langmuir waves, when $\omega/k > c$, happens with a higher increment than for $\omega/k \lesssim c$ (Machabeli *et al.* 2015). Such superluminal waves cannot be damped in the pulsar magnetosphere and the Langmuir oscillations are accumulated, which transfer energy along the magnetic field lines and finally into the Crab nebula.

It is important to estimate how big the energy losses can be before the waves reach the nebula. One of the most essential mechanisms of longitudinal wave–particle

https://doi.org/10.1017/S0022377816000416 Published online by Cambridge University Press

interaction in the weak-turbulence approximation is wave scattering by plasma particles. The resonance process can be described by the following expression:

$$\frac{\omega_{k\to 0} - k_c c}{k_{\to 0} - k_c c} = v. \tag{4.1}$$

Inserting frequencies from (3.9) and (3.11), we find that this process can only take place for the waves with the spectrum $\omega \approx k_c c$, which can be scattered on thermal particles of relativistic plasma.

One can introduce the plasma waves as a gas of quantum quasiparticles, the plasmons (which is the analogy to photons), and also the concept of the plasmon number. The number of plasmons is conserved through the scattering process

$$N_k = \frac{|E_k|^2}{\omega_k} \approx \text{const}. \tag{4.2}$$

The energy is pumped into the long-wavelength region $k \to 0$. From conservation of the quantity $|E_k|^2/\omega_k$, it follows that the energy transferred to the particles equals the following relation: $|E_{k=0}|^2/|E_k|^2 \approx \omega_{k=0}/\omega_k \approx \gamma^{-2}$. As one can see, the energy loss during this process is quite significant. This result was obtained earlier in the paper by Lominadze *et al.* (1979), where it was assumed that wave generation takes place in the subluminal region, $v_{ph} < c$. Contrary to this, in our case as it was shown above that the greatest part of the energy is generated in the region of frequencies $\omega_{k\to 0}$. Consequently, we should consider the nonlinear scattering of Langmuir waves on the particles for the region of wavenumbers where $v_{ph} \gg c$. Substituting the value for the frequency of electrostatic waves of relativistic plasma from expression (3.9) in the resonance condition for nonlinear scattering (4.1), we obtain

$$\frac{\omega_p}{\gamma_p^{3/2}} \left(\frac{1 + 3k^2c^2\gamma^2}{2\omega_p^2} - \frac{1 + 3k'^2c^2\gamma^2}{2\omega_p^2} \right) \frac{1}{k - k'} = v. \tag{4.3}$$

Considering that $k^2 - k'^2 = (k - k')(k + k')$ and $k \sim k'$, one can conclude that $v/c \approx 3\gamma_p^{1/2} c/v_{ph} \ll 1$. Such thermal particles practically do not exist in ultrarelativistic plasma, which makes the scattering process ineffective.

When propagating in the nebula direction the particle density reduces and consequently also ω_p^2. However, ω^2 should be conserved. In the non-relativistic case, it would mean that k^2 increases. For relativistic plasma, when $k \to 0$, the frequency $\omega \approx \omega_{LC}/\gamma_{LC}^{3/2}$. This makes it sufficient that

$$\left(\frac{n_{p_{LC}}}{n_{17}} \right)^{1/2} \left(\frac{\gamma_{LC}}{\gamma_p} \right)^{-3/2} \simeq 1, \tag{4.4}$$

where $n_{LC} \approx 10^{13}$ cm^{-3} is the density of the bulk plasma near the light cylinder, and within the fibres of the Crab nebula the plasma density $n_{17} \sim 10^3$ cm^{-3} (Manchester & Taylor 1977). The Langmuir waves are propagating from the light cylinder towards the nebula without changing the frequency. Therefore, the thermal particles of plasma should be cooled down to Lorentz factors $\sim$1, as follows from (4.4). One can conclude that long-wave ($k \to 0$) energy of transfer at distances $R_{17} \sim 10^{17}$ cm occurs practically without losses.

We have shown that the Crab nebula is constantly provided with energy, which is enough to explain its emission. This energy is concentrated in the so-called plasmon 'condensate', which is then followed by conversion of energy of the plasma oscillation into the kinetic energy of the particles. This particular issue is considered in the next section.

https://doi.org/10.1017/S0022377816000416 Published online by Cambridge University Press

5. Collapse of Langmuir waves

The plasmon 'condensate' is an intense gas of long-wave plasmons and appears to be unstable when the background modulation via low-frequency waves occurs. Such low-frequency waves do not exist in the pulsar magnetosphere, while magnetospheric plasma consists only of electrons and positrons. Differently from the magnetosphere, in the Crab nebula region the plasma also contains ions, which can easily lead to low-frequency modulation of the plasmon background that in its turn causes modulational instability (Vedenov & Rudakov 1964). Through the development of the mentioned instability cavities are formed, higher energy localization regions, and the energy of Langmuir waves is localized in the cavities. The plasmons appear to be captured inside such cavities; the high-frequency pressure displaces plasma particles out from the cavity, which causes its deepening and as a result more and more plasmons are captured inside it. The process of spatial contraction of cavities is accelerated, which is finally terminated by collapse of the cavities. This phenomenon cannot be considered in the weak-turbulence approximation. The collapse of Langmuir waves was considered in Zakharov (1972) and dynamics of collapse of cavities was studied in Galeev *et al.* (1977). The numerical experiment which was demonstrating the process of collapse was presented by Degtyarev *et al.* (1976). It was found that during the collapse process the wave vector $\boldsymbol{k}$ grows until the phase velocity of the waves equals the velocity of plasma particles, such particles come into resonance with waves and extract their energy. This happens through the Landau damping process, which stops the collapse of the cavities and results in the growth of a long tail of the particle distribution function (Pelletier 1982).

Heretofore, we were describing the collapse scenario that takes place in plasmas without an external magnetic field. In the Crab nebula the plasma density $n_0 \sim 10^3\ \mathrm{cm}^{-3}$ and the magnetic field $B_0 \sim 10^{-3}$ G; consequently, $\omega_p \gg \omega_B \equiv eB_0/mc$ and one can easily ignore the influence of the magnetic field on the process of collapse of Langmuir waves. In this case, the equation for the amplitude of Langmuir oscillations can be written in the following form:

$$\frac{\partial^2 E}{\partial t^2} - \frac{\omega_p^2}{\gamma_p^{3/2}} E - \frac{3r_D^2\omega_p^2}{\gamma_p^{3/2}} \frac{\partial^2 E}{\partial x^2} = \frac{\omega_p^2}{\gamma_p^{3/2}} \left(\frac{n}{n_0}\right) E, \tag{5.1}$$

where r_D is relativistic Debye radius. The perturbation of the particle density n caused by plasmon pressure satisfies the following equation:

$$\frac{\partial^2 n}{\partial t^2} - \left(\frac{T_e}{M}\right) \frac{\partial^2 n}{\partial x^2} = \frac{\pi M}{16} \frac{\partial^2}{\partial x^2} |E|^2, \tag{5.2}$$

where T_e is the electron temperature and M is the ion mass. The auto-model solution of the following equation reveals a 'burst'-like nature:

$$|E|^2 \sim \frac{E_0^2}{(\tau_0 - \tau)^2}. \tag{5.3}$$

Here $\tau \equiv n_0 T_e(\omega_p/\gamma_p^{3/2}) t E_0^2/(8\pi)$, E_0^2 is the energy density of the waves at the initial moment of the modulational instability and τ_0 is the time of the collapse active phase (Zakharov 1972). During the collapse process, the electric field of the waves is reduced at the expense of growth of the kinetic energy of the resonant particles.

https://doi.org/10.1017/S0022377816000416 Published online by Cambridge University Press

6. Synchrotron emission of the Crab nebula

In 1953, I.S. Shklovsky had assumed that the continuous radio emission of the nebula is generated through the synchrotron-radiation mechanism (Shklovsky 1953). Soon after that, observations of the nebula in the optical domain revealed a very high percentage of the linear polarization (Dombrovsky 1954; Vashakidze 1954; Oort & Warvalen 1956). The variation of the polarization degree in different regions confirms the leading role of the synchrotron radiation as the mechanism of generation of the nebular emission. In the works by Gould (1965), Weekes *et al.* (1989), de Jager *et al.* (1996), it was proposed that the spectra are formed through the synchro-Compton emission mechanism. Above hundreds of MeV the intensity of the synchrotron emission is strongly suppressed and beginning from GeV energies the emission is generated via inverse-Compton scattering. We will be considering emission up to the MeV energy range and therefore will only investigate the synchrotron radiation. However, the problem of pulsar rotation energy transfer to the nebula is equally important also for the radiation that is generated through the inverse-Compton mechanism.

As mentioned above, the modulational instability is developed in the Crab nebula that produces cavities, which contain the energy of long-wavelength electrostatic oscillations. Eventually the cavities are undergoing collapse. At the initial stage of the collapse process, the rate of the process is defined by the value of the increment of modulational instability. Later, when $\tau \to \tau_0$ (see (5.3)), the collapse rate increases with a burst-like behaviour and begins the active phase of the process. At this stage the damping of the energy of Landau waves through the Landau damping process on the cavity particles starts to be essential, which results in the particles accelerating up to very high Lorentz factors and the collapse process stops. The characteristic size of the cavity during the active phase is estimated to be a few Debye radii (Arcimowich & Sagdeev 1979).

For the bulk of the plasma of the Crab nebula the particle number density $n_0 \sim 10^3$ (Manchester & Taylor 1977) and the Lorentz factors $\gamma_p \sim 1$ prior to re-acceleration in the nebula region. According to the observations, the maximum energy comes on the soft X-rays. Hence, one can assume that the majority of the particles of bulk plasma were accelerated up to Lorentz factors of the order of 5×10^6. For such particles the frequency of the synchrotron emission comes in the desired domain

$$\omega_s = (eB/mc)\gamma^2 = 1.8 \text{ keV}. \tag{6.1}$$

Now, if we calculate the Debye radius, $r_D = \gamma_p^{3/2} c/\omega_p = 5 \times 10^{14}$ cm and an average distance between the plasma particles $r_p \approx n^{-1/3} \sim 10^{-1}$ cm. Consequently, the maximum number of particles in the Debye volume can be estimated as follows: $N_D \approx (r_D/r_p)^3 \sim 10^{46}$.

The particles from the tail of the plasma distribution function also take part in the process of the cavity collapse, which are accelerated up to $\gamma_s \sim 3 \times 10^9$ (Mahajan *et al.* 2013). Such particles when radiating through the synchrotron regime emit photons in the domain of 100 MeV (estimated from (6.1)). Assuming that $n_p\gamma_p = n_s\gamma_s$, we find the number of the particles $N_s \sim 10^{38}$. This value is close to one found from observations (Aliu *et al.* 2014). Multiplying the number of the particles by the radiation power of a single particle, we get

$$\left(\frac{\mathrm{d}\varepsilon}{\mathrm{d}t}\right)_s = \left(\frac{2e^2\omega_B^2}{3c}\right)\gamma^2. \tag{6.2}$$

https://doi.org/10.1017/S0022377816000416 Published online by Cambridge University Press

Consequently, the power of the synchrotron emission at the energies of the order of 100 MeV equals

$$\left(\frac{\partial \varepsilon}{\partial t}\right)_s \approx 10^{36} \text{ erg s}^{-1}. \tag{6.3}$$

The wavelength of the electrostatic waves cannot be less than the value of r_D, since in the volume with the size of the order of the Debye radius the electric field is screened due to the grouping of the charged particles that causes the medium polarization.

7. High frequency emission spectra of the Crab nebula

The problem of defining the particle distribution function that is formed through the collapse process was considered for the non-relativistic case (Galeev *et al.* 1977; Pelletier 1982). The energy dissipation of Langmuir perturbations into the short-wavelength region inside the isothermal plasma is caused by resonant absorption on the plasma particles. The process dynamics in this regime is described by two quasilinear equations for the particle distribution function $f_0(p)$ and the continuity equation for the energy flux

$$\frac{\partial |E_k|^2}{\partial t} + \frac{\partial}{\partial \boldsymbol{k}}\left(|E_k|^2 \frac{\mathrm{d}k}{\mathrm{d}t}\right) - 2\Gamma_k |E_k|^2 = 0. \tag{7.1}$$

One should consider three different regions when calculating spectra: source, inertial interval and absorption region (Kolmogorov 1941; Heisenberg 1948). The collapse of the cavity ceases the process of wave-energy damping on the particles, which means that in (7.1) the first and the last terms compensate each other and the energy flux by spectrum is conserved, like in the region of the inertial interval during the wave splitting from big to small scales, $|E_k|^2 \mathrm{d}k/\mathrm{d}t = A$, where $A \neq f(\boldsymbol{k})$. Consequently,

$$|E_k|^2 = A\frac{\mathrm{d}t}{\mathrm{d}k} \sim \frac{t}{k}. \tag{7.2}$$

It is assumed that the number of plasmons inside the cavity is a constant value, $V|E_k|^2 = \text{const.}$, $V \sim R^3$ is the cavity volume and

$$|E_k|^2 \sim \frac{1}{R^3}. \tag{7.3}$$

The quantity $|E_k|^2$ grows with time with a burst-like behaviour; therefore, $t \sim (t_0 - t)$ and $|E_k|^2 \sim t^{-2}$ (5.3). Taking into account that $k \sim 1/R$ from (7.3), we will find $t \sim k^{-3/2}$. Substituting this value for t into (7.2), we find (Arcimowich & Sagdeev 1979)

$$|E_k|^2 \sim k^{-5/2}. \tag{7.4}$$

The active phase of the cavity collapse process is followed by quasilinear interaction of Langmuir oscillations with the particles. The quasilinear integral is conserved during this process. In the region where these processes develop, the magnetic field is negligible and the medium is isotropic. Consequently, it is more convenient to write the quasilinear integral in spherical coordinates. The electrostatic perturbation $\boldsymbol{E} \parallel \boldsymbol{k}$ and the particles move in the direction of the wave electric field; consequently, $\boldsymbol{k} \parallel \boldsymbol{v}$. After integrating by angles, we get

$$\frac{\partial}{\partial t}\left\{f + k^2 p^2 \frac{|E_k|^2}{2\delta_k}\frac{\partial f}{\partial p}\right\} = 0 \tag{7.5}$$

https://doi.org/10.1017/S0022377816000416 Published online by Cambridge University Press

and finally

$$f + k^2 p^2 \frac{|E_k|^2}{2\delta_k} \frac{\partial f}{\partial p} = C. \tag{7.6}$$

Here C is a constant value and δ_k is the decrement of Langmuir wave absorption. As mentioned before, at the initial stage of the development of instability the rate of the collapse defines the increment of the modulational instability. Later, when $t \to t_0$, the collapse process obtains the burst-like behaviour and the process enters the active phase. At this stage the cavity particles effectively absorb energy of Langmuir waves. As a result, particles are accelerated up to high Lorentz factors. The cavity collapse stops when in the region of resonant particles the distribution function forms a plateau. However, another scenario of development of these processes is still possible if the initial energy of waves is not sufficient for forming the plateau. In this case the system cannot reach the stationary state and the wave field will be completely absorbed by particles. Through the wave-energy absorption the loss of the momentum by plasmons results in the growth of the momentum of resonant particles. Therefore, we assume that $kp = \text{const.}$ or

$$k^{-1} \to p. \tag{7.7}$$

The dispersion relation for electrostatic waves in relativistic plasma has the following form:

$$\varepsilon(\omega) = 1 - \Sigma_a \frac{\omega_a^2}{\omega} \int \left(\frac{\mathrm{d}f_{0_a}}{\mathrm{d}\boldsymbol{p}} \right) \frac{\boldsymbol{v_a}}{c} \frac{1}{\omega - \boldsymbol{k}\boldsymbol{v_a}} \mathrm{d}\boldsymbol{p} = \boldsymbol{0}; \tag{7.8}$$

summation should be produced by plasma particles, plasma electrons and positrons – p, electrons of primary beam – b and ions – i, $\omega_a^2 = 4\pi e^2 n_a / m_a$ and n_a is the particle number density. Let us introduce the frequency in the following way, $\omega = \omega_0 + \mathrm{i}\delta_k$ ($|\delta_k| \ll \omega_0$), and multiply and divide the integrand expression by $(\omega - \mathrm{i}\delta_k)$. This will give us the real and imaginary parts of $\varepsilon(\omega)$, which can be equated to zero. One can perform the integration by parts of the real part of $\varepsilon(\omega)$, which gives

$$\mathrm{Re}\varepsilon(\omega_0) = 1 - \Sigma_a \omega_{p_a}^2 \int f_{0_a} \mathrm{d}p \frac{(\omega - k v_a)^2}{\gamma^3}. \tag{7.9}$$

Prior to collapse, the plasma energy is mainly in plasmon gas. Due to cavity collapse the energy of Langmuir waves is pumped into particles through the Landau damping, re-accelerating them up to high Lorentz factors. This happens when the resonance condition $\omega - k v_a = 0$ is fulfilled. In the region of subluminal velocities, the frequency can be introduced as $\omega_0 \approx kc$ and the velocity $v_a \approx c(1 - 1/2\gamma_a^2)$. Inserting these expressions into (7.9), we obtain

$$\mathrm{Re}\,\varepsilon(\omega_0) = 1 - \frac{2\gamma_b \omega_{b_e}^2}{k^2 c^2}. \tag{7.10}$$

The dielectric permittivity for the longitudinal waves is written as

$$\left.\begin{aligned} \varepsilon(\omega) &= \mathrm{Re}\varepsilon + \mathrm{i}\mathrm{Im}\,\varepsilon, \\ \varepsilon(\omega_0 + \mathrm{i}\delta_k) &\approx \varepsilon(\omega_0) + \mathrm{i}\delta_k \frac{\partial \mathrm{Re}\varepsilon(\omega_0)}{\partial \omega_0}. \end{aligned}\right\} \tag{7.11}$$

https://doi.org/10.1017/S0022377816000416 Published online by Cambridge University Press

Equating the imaginary parts gives

$$\delta_k = \mathrm{Im}\,\varepsilon(\omega_0) \Big/ \frac{\partial \mathrm{Re}\varepsilon(\omega_0)}{\partial \omega_0}. \tag{7.12}$$

For obtaining the final expression for the decrement, let us first find $\mathrm{Im}\,\varepsilon(\omega_0)$. We make the following change, $\mathrm{d}f_0/\mathrm{d}\boldsymbol{p} \rightarrow (\mathrm{d}f_0/\mathrm{d}\boldsymbol{v})(\partial \boldsymbol{v}/\partial \boldsymbol{p})$, in (7.8) and rewrite this equation as

$$1 - \sum_a \frac{\omega_a^2}{\omega} \int \frac{\mathrm{d}f_{0_a}}{\mathrm{d}\boldsymbol{v}} \frac{\boldsymbol{v}_a}{c} \frac{1}{\omega - \boldsymbol{k}\boldsymbol{v}_a} \mathrm{d}\boldsymbol{v} = 0. \tag{7.13}$$

After using a well-known formula $\{\delta_k/[(\omega_0 - kv)^2 - \delta_k^2]\} = \mathrm{i}\pi\delta(\omega_0 - kv)$, which is valid for the following condition: $(\omega_0 - kv)^2 \gg \delta_k^2$ (where $\delta(\omega_0 - kv)$ is the Dirac function), from (7.12) we finally find

$$\delta_k \sim \frac{k}{\gamma} \left(\frac{\partial f_0}{\partial v} \right) |_{v \approx c}. \tag{7.14}$$

We need to find the value for C in (7.6) at the moment when the cavity collapse finishes. Let us consider the case when the wave initial energy is not sufficient for forming the plateau, the stationary state cannot be reached and the wave energy is entirely absorbed on the particles. In this case $C = f \sim p^{-s}$. Using the expressions (7.4) and (7.7), we get $k^{-5/2} \rightarrow (mc\gamma)^{5/2}$. When $p/mc \gg 1$, $\gamma \sim p$. From (7.6), we will finally get

$$f_0 \sim \int \gamma^{-9/2-s}\, \mathrm{d}\gamma = \gamma^{-7/2-s}. \tag{7.15}$$

Until the wave initial energy is not entirely expended, the quasilinear diffusion tries to form the plateau in the region of wave–particle interaction. Therefore, one could expect that $s \ll 1$ and neglect this term. It should be mentioned that for the non-relativistic case, there was obtained $f_0 \sim v^{-7/2}$ (Galeev *et al.* 1977; Pelletier 1982).

The index of the power-law spectrum of the synchrotron emission is defined by the following expression (Ginzburg 1981):

$$\alpha = \frac{\beta - 1}{2}, \tag{7.16}$$

where β is the index of the power of the particle distribution function. From (7.15), $f_0 \sim \gamma^{-\beta} \approx \gamma^{-7/2}$. Inserting the value for β into (7.16) for the emission spectrum power-law index, we find

$$\alpha \sim 5/4, \tag{7.17}$$

which well corresponds to the observational data of the high-frequency radiation of the Crab nebula (Manchester & Taylor 1977).

8. Conclusion

We assumed that one of the central problems when investigating the Crab nebula is finding the mechanism providing transfer of the rotation energy of the PSR 0531+21 pulsar to the nebula. This problem consists of several steps, which have been considered and published at different times by the authors of the present work. In this paper we have collected all of the previous works, processed them and

https://doi.org/10.1017/S0022377816000416 Published online by Cambridge University Press

presented them with a single point of view. The high-energy spectrum of the Crab nebula is first calculated in this paper, as a result of the presented model for the nebula emission. The good correspondence of the spectral index with the observations indicates the consistency of the presented scenario.

Here we list the major results of our investigations.

(1) The problem of a relativistic particle moving along a rotating rigid string was considered in detail (Machabeli & Rogava 1994). The same problem was also considered from the point of view of energy conservation and momentum conservation laws. It was shown that after defining the momentum, the system ceases to be closed and the entire rotational energy is transferred to the particle (Machabeli *et al.* 1996).

(2) These papers are the basis of the following works considering the pulsar rotational energy pumping into the electrostatic waves of magnetospheric plasma. It was shown that the periodical change of the motion of the particle flux results in the pulsar's rotational energy pumping into the Langmuir oscillations (Machabeli *et al.* 2005; Mahajan *et al.* 2013; Machabeli *et al.* 2015).

(3) We have performed the estimation of the possibility of an idealized mechanism of rotational energy pumping. From equation (18), it follows that the considered mechanism gives the possibility to consume much more power than is needed for explaining the emission intensity of the nebula. We assume that restriction of the power with the value 5×10^{38} erg s^{-1} is caused by reconstruction of the magnetic field in the magnetosphere from dipolar to poloidal (Michel 1969; Machabeli *et al.* 2000; Bogovalov 2001; Rogava *et al.* 2003; Osmanov *et al.* 2008). It was demonstrated that the magnetic field lines after the light-cylinder region transform into the Archimedes spiral with the step that provides the force-free regime, when the particles do not feel the influence of the magnetic field and, consequently, the rotation of the pulsar.

(4) The plasma mechanism of generation of drift waves and the growth of magnetic perturbations across the pulsar magnetic field was considered, which causes the magnetic field reconstruction near the light cylinder. This process consumes only a small fraction of the pulsar's rotational energy.

(5) It is shown that the pulsar rotation energy is mainly pumped into the long-wave Langmuir oscillations, where the wave phase velocity exceeds the speed of light. There are no particles with such speed and the waves cannot be damped. As a result, the condensate of electrostatic oscillations is formed (Machabeli *et al.* 2015). This plasmon condensate is transferred into the nebula practically without any energy losses.

(6) Differently from the pulsar magnetosphere, the nebula also contains ions. Therefore, there exist low-frequency electrostatic oscillations, particularly ion sound. This fact ensures the development of the modulational instability and finally the Langmuir waves collapse.

(7) Through the Langmuir wave collapse the scale of the wavelength becomes smaller and, consequently, reduces the wave phase velocity. As soon as the phase velocity becomes smaller than the speed of light, the mechanism of Landau damping is switched on. As a result, waves transfer their energy to the particles. The particles are accelerated and form the particle spectrum, which is calculated by taking into account the influence of the collapse process on the wave absorption. The re-accelerated particles re-emit the energy of the Langmuir waves, which we detect as the high-frequency emission of the nebula. The spectral index of the synchrotron emission obtained from theoretical calculation matches well with the observed one.

https://doi.org/10.1017/S0022377816000416 Published online by Cambridge University Press

Acknowledgement

The research was partially supported by the Shota Rustaveli National Science Foundation (grants N31/49 and FR/516/6-300/14).

Appendix A. Additional peculiarities of centrifugal deceleration

In 1994, Machabeli & Rogava have suggested and studied a relatively simple gedanken experiment (Machabeli & Rogava 1994): a straight pipe, rotating around an axis normal to its symmetry axis, and a small bead, moving inside the pipe without friction. The pipe rotates in a horizontal plane, with a constant angular velocity $\omega = \text{const.}$, and is supposed to be massless and absolutely rigid. It was assumed that at $t = 0$ the bead is above the rotator's pivot ($r_0 = 0$) and has an initial velocity v_0. The dynamics of the bead was considered in the non-inertial frame of reference of the rotating pipe (RNF). It was found that the acceleration of the bead is not always positive; in certain cases its motion has a decelerating nature.

The highly surprising behaviour of the bead was interpreted in terms of reversal in direction of a centrifugal force (Machabeli & Rogava 1994). The interpretation was disputed (Miller & Abramovicz 1994); it was recommended to define the relativistic centrifugal force in a way which would exclude the 'reversal' of the force and it was argued that the deceleration could be ascribed to the relativistic mass variation. Yet another alternative interpretation was suggested by de Felice. In particular, relativistic dynamics on a rotating disk was considered and for the case of radially constrained motion the disappearance of the bead's radial velocity at the light cylinder was interpreted as the result of an infinite Doppler shift experienced by the inertial observer (de Felice 1995). Both these studies acknowledged that, as had been stated in Machabeli & Rogava (1994), the 'pipe + bead' gedanken experiment is highly idealized and there certainly is no real 'bounce' of the bead at the light cylinder. However, both these studies also confirmed the main result of Machabeli & Rogava (1994): a centrifugally driven particle can move with negative acceleration; it can exhibit a decelerating mode of motion.

Revisiting this problem, we would like to point out a few interesting aspects of the dynamics of a centrifugally driven particle, which had not been described in Machabeli & Rogava (1994). These additional oddities, related with the gedanken experiment, highlight once again the paradoxical possibility of decelerating motion of the centrifugally driven particle.

It turns out that the main results of Machabeli & Rogava (1994) are not related at all with the choice of the frame in which the problem is considered. In particular, considering the bead motion in the laboratory inertial frame (LIF) of reference, relative to which the pipe rotates, we found that the decelerating character of the motion can be derived in exactly the same way. Two more interesting aspects of the problem are quite surprising and remarkable analogies between the results of Machabeli & Rogava (1994) and: (1) rotational motion of a classical mathematical pendulum, (2) radial geodesic motion of a test particle in Schwarzschild geometry. Both of them are briefly discussed in the following subsections of this appendix.

A.1. *LIF treatment and pendulum analogy*

We study motion of the bead in the LIF, where a spacetime is Minkowskian. Owing to the polar symmetry of the experimental setup it is useful to write the spatial part of the metric in polar coordinates:

$$\mathrm{d}s^2 \equiv -\mathrm{d}\tau^2 = -\mathrm{d}t^2 + r^2\,\mathrm{d}\varphi^2 + \mathrm{d}r^2, \tag{A 1}$$

https://doi.org/10.1017/S0022377816000416 Published online by Cambridge University Press

where τ is a proper time of the bead. We use geometric units with $G = c = 1$. The metric has three non-zero Christoffel symbols:

$$\Gamma^{r}_{\phi\phi} = -r, \quad \Gamma^{\phi}_{r\phi} = \Gamma^{\phi}_{\phi r} = 1/r, \tag{A 2.a,b}$$

The radial and angular velocities of a particle are defined as

$$v \equiv \mathrm{d}r/\mathrm{d}t, \quad \omega \equiv \mathrm{d}\phi/\mathrm{d}t, \tag{A 3a,b}$$

while the Lorentz factor is

$$\gamma \equiv \mathrm{d}t/\mathrm{d}\tau = (1 - r^2\omega^2 - v^2)^{-1/2}. \tag{A 4}$$

The motion of the bead is free in the radial direction, while the pipe wall acts on the bead with tangential force of reaction. The radial component of the equation of motion,

$$\frac{\mathrm{d}^2 r}{\mathrm{d}\tau^2} + \Gamma^{r}_{\alpha\beta}\left(\frac{\mathrm{d}x^{\alpha}}{\mathrm{d}\tau}\frac{\mathrm{d}x^{\beta}}{\mathrm{d}\tau}\right) = 0, \tag{A 5}$$

by taking into account (A 2)–(A 4), is reduced to

$$\frac{\mathrm{d}^2 r}{\mathrm{d}\tau^2} = r\left(\frac{\mathrm{d}\phi}{\mathrm{d}\tau}\right)^2 = \omega^2 r\gamma^2. \tag{A 6}$$

Since $\mathrm{d}r/\mathrm{d}\tau = \gamma v$ and

$$\frac{\mathrm{d}\gamma}{\mathrm{d}t} = \gamma^3 v\left(\omega^2 r + \frac{\mathrm{d}v}{\mathrm{d}t}\right), \tag{A 7}$$

it is easy to find that

$$\frac{\mathrm{d}^2 r}{\mathrm{d}\tau^2} = \gamma^2\left[(1 + \gamma^2 v^2)\frac{\mathrm{d}^2 r}{\mathrm{d}t^2} + \omega^2 r\gamma^2 v^2\right]. \tag{A 8}$$

Using (A 4) again, we can see that

$$1 - \gamma^2 v^2 = \gamma^2(1 - r^2\omega^2 - 2v^2), \tag{A 9}$$

$$1 + \gamma^2 v^2 = \gamma^2(1 - r^2\omega^2), \tag{A 10}$$

which implies that

$$\frac{\mathrm{d}^2 r}{\mathrm{d}t^2} = \frac{\omega^2 r}{1 - \omega^2 r^2}\left(1 - \omega^2 r^2 - 2v^2\right). \tag{A 11}$$

This is exactly the same equation which was derived in Machabeli & Rogava (1994) for the radial acceleration of the bead as measured in RNF. This equation also can be written in the following, surprisingly elegant, form:

$$\frac{\mathrm{d}^2 r}{\mathrm{d}t^2} = \left(\frac{1 - \gamma^2 v^2}{1 + \gamma^2 v^2}\right)\omega^2 r, \tag{A 12}$$

https://doi.org/10.1017/S0022377816000416 Published online by Cambridge University Press

which distinctly shows asymptotic peculiarities of the bead motion: if the motion is non-relativistic ($\gamma v \ll 1$), it reduces to the usual classical equation for centrifugal acceleration: $\mathrm{d}^2r/\mathrm{d}t^2 = \omega^2 r$, while in the ultrarelativistic limit ($\gamma v \gg 1$) the sign of the right-hand side of (A 12) changes to the opposite: $\mathrm{d}^2r/\mathrm{d}t^2 = -\omega^2 r$. Note, furthermore, that when $\gamma_0 v_0 = 1$ ($v_0 = \sqrt{2}/2$), the remarkable sign reversal occurs from the very beginning of the motion.

Note that (A 11) can be rewritten as a differential equation for the function $y \equiv v^2(r)$. The resulting equation is

$$\frac{\mathrm{d}^2 y}{\mathrm{d}t^2} + \frac{4\omega^2 r}{1-\omega^2 r^2} y = 2\omega^2 r, \tag{A 13}$$

with the solution, which can be written as

$$y(r) = (1-\omega^2 r^2) + \text{const.} \quad (1-\omega^2 r^2)^2. \tag{A 14}$$

In particular, for the case when initially ($t = 0$) the bead is situated on top of the pivot $r_0 = 0$ and has a velocity v_0, (A 14) implies that const. $= v_0^2 - 1$. Therefore, for the function $v(r)$ we obtain the result derived in Machabeli & Rogava (1994):

$$v(r) = \sqrt{(1-\omega^2 r^2)\left[1 - \frac{(1-\omega^2 r^2)}{\gamma_0^2}\right]}. \tag{A 15}$$

Yet another interesting point is that if one introduces new variables: $\phi \equiv 2\arccos(\omega r)$, $\lambda \equiv \omega t$ and $\Omega^2 \equiv 1 - v_0^2$, we can reduce the equation of motion to the following, remarkably simple, equation:

$$\frac{\mathrm{d}^2\phi}{\mathrm{d}\lambda^2} + \Omega^2 \sin\phi = 0. \tag{A 16}$$

It is the well-known pendulum equation, describing nonlinear oscillations of a free mathematical pendulum. One can easily derive (A 16) from (A 15) by rewriting it in the above-introduced notation as $\mathrm{d}\phi/\mathrm{d}\lambda = -2\sqrt{1-\Omega^2\sin^2(\phi/2)}$, and taking one more derivative by λ.

With this analogy, the striking resemblance of the solutions of Machabeli & Rogava (1994) with mathematical pendulum motion becomes more transparent. If we introduce the concept of an 'analogous pendulum', governed by (A 16), then the initial conditions ($r_0 = 0$, $(\mathrm{d}r/\mathrm{d}t)_{t=0} = v_0$) are replaced by $\phi_0 = \pi$ and $(\mathrm{d}\phi/\mathrm{d}\lambda)_{\lambda=0} = -2v_0$. The analogous pendulum rotates in a vertical plane with the effective frequency Ω. The time interval needed by the bead to reach the $\omega r = 1$ 'light cylinder' corresponds to the time needed by the analogous pendulum to reach its stable equilibrium ($\phi = 0$) point. This time interval is finite, as it, certainly, should be.

A.2. *The Schwarzschild analogy*

One can show that this problem is also in an unusual analogy with a certain kind of geodesic motion in Schwarzschild geometry. Let us consider a radial geodesic 'fall' of a test particle onto a Schwarzschild black hole with mass M. Let a radial velocity of the particle at infinity be V_∞ and pointed inwards. If one denotes by $E = \gamma_\infty \equiv$

https://doi.org/10.1017/S0022377816000416 Published online by Cambridge University Press

$(1 - V_\infty{}^2)^{-1/2} > 1$ the specific energy of the particle per its rest mass, then for its radial velocity relative to the observer at infinity $V_{\hat{r}} \equiv \sqrt{g_{rr}}\,\mathrm{d}r/\mathrm{d}t$ one gets

$$V_{\hat{r}}{}^2 = \frac{E^2}{4} - \left[\frac{E}{2} - \frac{1}{E}\left(1 - \frac{2M}{r}\right)\right]^2 \tag{A 17}$$

(see e.g. McVittie (1956), where this equation is written in different notation). For the quantity $\mathrm{d}V_{\hat{r}}/\,\mathrm{d}t$ (called by McVittie the 'nontensor radial acceleration of the particle'), one gets

$$\frac{\mathrm{d}V_{\hat{r}}}{\mathrm{d}t} = \frac{2M}{Er^2}\left[\frac{E}{2} - \frac{1}{E}\left(1 - \frac{2M}{r}\right)\right]\sqrt{1 - \frac{2M}{r}}. \tag{A 18}$$

One can see that the acceleration of the particle is negative (i.e. the modulus of the particle's infall velocity is increasing), until the particle reaches the radial distance $r_1 = 4M/(2 - \gamma_\infty{}^2)$, where the acceleration changes its sign, and $V_{\hat{r}}$ reaches its maximum velocity $V_{max} = \gamma_\infty/2$. More precisely, we have the following regimes of the motion:

(1) $V_\infty \ll 1$ ($\gamma_\infty \approx 1$): the particle begins to move with increasing speed, at $r_1 \approx\!= 4M$ reaching its maximum value ($V_{max} \approx 1/2$) and decelerates, afterwards, down to zero radial velocity, when the particle approaches the black-hole horizon $r \to 2M$;

(2) $V_\infty = \sqrt{2}/2$, ($\gamma_\infty = \sqrt{2}$): the 'threshold' case; with $\mathrm{d}V_{\hat{r}}/\mathrm{d}t = 0$ ($V_{max} = V_\infty$, $r_1 \to \infty$), and the particle decelerating smoothly down to the horizon;

(3) $V_\infty > \sqrt{2}/2$: the acceleration is positive during the whole course of the motion – the motion is decelerating all the time.

This scenario remarkably resembles (even quantitatively) the one in Machabeli & Rogava (1994) gedanken experiment. This likeness happens due to the remarkable similarity between (A 17) and the corresponding equation for $\mathrm{d}r/\mathrm{d}t$ from Machabeli & Rogava (1994), which may be written as

$$\left(\frac{\mathrm{d}r}{\mathrm{d}t}\right)^2 = \frac{E^2}{4} - \left[\frac{E}{2} - \frac{1}{E}\left(1 - \omega^2 r^2\right)\right]^2. \tag{A 19}$$

The resemblance is a manifestation of likeness of the spacetime in the rotating pipe:

$$\mathrm{d}s_p{}^2 = -(1 - \omega^2 r^2)\,\mathrm{d}t^2 + \mathrm{d}r^2 \tag{A 20}$$

with the Schwarzschild spacetime along a radial geodesic ($\theta = \text{const.}$, $\varphi = \text{const.}$)

$$\mathrm{d}s_s^2 = -(1 - 2M/r)\,\mathrm{d}t^2 + \frac{\mathrm{d}r^2}{1 - 2M/r}. \tag{A 21}$$

Comparing, for example, lapse functions for these two metrics ($\alpha_p \equiv \sqrt{-g_{tt}} = \sqrt{1 - \omega^2 r^2}$ and $\alpha_s \equiv \sqrt{-g_{tt}} = \sqrt{1 - 2M/r}$), one can see that α_p and α_s become infinite at the light cylinder and horizon, respectively. Obviously, the likeness is not complete: the spatial part of the rotating pipe metric is flat, while the spatial part of (A 22) metric is curved ($g_{rr} \neq 1$). The latter difference is also essential: it ensures finiteness of the time t^* (Machabeli & Rogava 1994) needed by the bead to reach the light cylinder $R_L \equiv \omega^{-1}$. As is well known, an analogous time interval for the test particle to reach the Schwarzschild black-hole horizon, as measured by the distant observer, is infinitely long.

https://doi.org/10.1017/S0022377816000416 Published online by Cambridge University Press

REFERENCES

ABRAMOWITZ, M. & STEGUN, I. A. (Eds) 1965 *Handbook of Mathematical Functions with Formulas, Graphs, and Mathematical Tables*, National Bureau of Standards Applied Mathematics Series, vol. 55. US GPO.

ALIU, E., ARCHAMBAULT, S., AUNE, T. *et al.* 2014 A search for enhanced very high energy gamma-ray emission from the 2013 March Crab nebula flare. *Astrophys. J.* **781**, L11–L17.

ARCIMOWICH, L. A. & SAGDEEV, R. Z. 1979 Physics of plasmas for physicists (in Russian). Atomizdat.

ARONS, J. 1981 Pulsar theory: particle acceleration and photon emission in the polar flux tube. In *Proceedings of the Varenna Summer School and Workshop on Plasma Astrophysics* (ed. T. D. Guenne & G. Levy), ESA SP-161, pp. 273–277.

BOGOVALOV, S. 2001 Magnetocentrifugal acceleration of plasma in a nonaxisymmetric magnetosphere. *Astron. Astrophys.* **367**, 159–169.

COCKE, W. J. 1975 On the production of power-law spectra and the evolution of cosmic synchrotron sources – a model for the Crab nebula. *Astrophys. J.* **202**, 773–781.

DEGTYAREV, L. M., ZAKHAROV, V. E. & RUDAKOV, L. I. 1976 Two examples of Langmuir wave collapse. *Phys. Plasmas* **2**, 438–447; (in Russian).

DEUTSCH, A. J. 1955 The electromagnetic field of an idealized star in rigid rotation in vacuo. *Rev. Mod. Phys.* **38**, 626–633.

DOMBROVSKY, V. A. 1954 O prirode izluchenia Krabovidnoi tumannosti. *Dokl. Akad. Nauk USSR* **94**, 1021–1032; (in Russian).

ERBER, T. 1966 High-energy electromagnetic conversion processes in intense magnetic fields. *Astron. Astrophys.* **38**, 626–659.

DE FELICE, F. 1995 Dynamics on a rotating disk. *Phys. Rev.* A **52**, 3452–3456.

GALEEV, A. A., SAGDEEV, R. Z., SHAPIRO, V. D. & SHEVCHENKO, V. I. 1977 Langmuir turbulence and dissipation of high-frequency energy. *Zh. Eksp. Teor. Fiz.* **73**, 1352–1369.

GINZBURG, V. L. 1981 *Teoreticheskaya fizika i astrofizika*. Nauka.

GINZBURG, V. L. & USOV, V. V. 1972 Concerning the atmosphere of magnetic neutron stars (pulsars). *J. Expl. Theor. Phys.* **15**, 280–284.

GOLDREICH, P. & JULIAN, W. H. 1969 Pulsar electrodynamics. *Astrophys. J.* **157**, 869–880.

GOULD, R. 1965 High-energy photons from the Compton–synchrotron process in the Crab nebula. *Phys. Rev. Lett.* **15**, 577–579.

HEISENBERG, W. 1948 Zur statistischen Theorie der Turbulenz. *Physica* **124**, 628–657.

DE JAGER, O., HARDING, A. K., MICHELSON, P. F., NEL, H. I., NOLAN, P. I., SEEKUMAR, P. & THOMPSON, D. J. 1996 Gamma-ray observations of the Crab nebula: a study of the synchro-Compton spectrum. *Astrophys. J.* **457**, 253–263.

KLEPIKOV, N. P. 1954 Izluchenie fotonov v elektronno-pozitronnoi plazme. *J. Expl. Theor. Phys.* **26**, 19–34; (in Russian).

KOLMOGOROV, A. 1941 The local structure of turbulence in incompressible viscous fluid for very large Reynolds numbers. *Dokl. Akad. Nauk SSSR* **30**, 301–316.

LOMINADZE, D. G., MIKHAILOVSKII, A. B. & SAGDEEV, R. Z. 1979 Langmuir turbulence of a relativistic plasma in a strong magnetic field. *J. Expl. Theor. Phys.* **50**, 927–939.

MACHABELI, G. Z., MCHEDISHVILI, G. Z. & SHAPAKIDZE, D. E. 2000 Force-free rotator. *Astrophys. Space Sci.* **271**, 277–292.

MACHABELI, G. Z., NANOBASHVILI, I. S. & ROGAVA, A. D. 1996 Centrifugal acceleration surprises. *Radiophys. Quant. Electron.* **39**, 26–30.

MACHABELI, G., OSMANOV, Z. & MAHAJAN, S. 2005 Parametric mechanism of the rotation energy pumping by a relativistic plasma. *Phys. Plasmas* **12**, 062906.

MACHABELI, G. & ROGAVA, A. 1994 Centrifugal force: a gedanken experiment. *Phys. Rev.* A **50**, 98–103.

MACHABELI, G., ROGAVA, A. & SHAPAKIDZE, D. 2015 On the origin and physics of gamma flares in Crab nebula. *Astrophys. J.* **814**, 38M–44M.

MACHABELI, G. Z. & USOV, V. V. 1989 Cyclotron instability and the generation of radio emission in pulsar magnetospheres. *Sov. Astron. Lett.* **15**, 393–397.

https://doi.org/10.1017/S0022377816000416 Published online by Cambridge University Press

MAHAJAN, S., MACHABELI, G., OSMANOV, Z. & CHKHEIDZE, N. 2013 Ultra high energy electrons powered by pulsar rotation. *Nat. Sci. Rep.* **3**, 1262–1268.

MANCHESTER, R. & TAYLOR, J. 1977 *Pulsars*. Freeman.

MCVITTIE, G. C. 1956 *General Relativity and Cosmology*. Chapman and Hall.

MICHEL, F. C. 1969 Relativistic stellar-wind torques. *Astrophys. J.* **158**, 727–738.

MICHEL, F. C. 1982 Theory of pulsar magnetospheres. *Rev. Mod. Phys.* **54**, 1–66.

MILLER, J. C. & ABRAMOWICZ, M. A. 1994 Comment on 'Centrifugal force: a gedanken experiment'. *SISSA ref. 178/94/A* 1–4.

OORT, J. H. & WARVALEN, T. 1956 Polarization and composition of the Crab nebula. *Bull. Astron. Inst. Neth.* **12**, 285–294.

OSMANOV, Z. 2011 The influence of corotation on high-energy synchrotron emission in Crab-like pulsars. *Mon. Not. R. Astron. Soc.* **411**, 973–977.

OSMANOV, Z., DALAKISHVILI, G. & MACHABELI, G. 2008 On the reconstruction of a magnetosphere of pulsars nearby the light cylinder surface. *Mon. Not. R. Astron. Soc.* **383**, 1007–1014.

OSMANOV, Z., MAHAJAN, S., MACHABELI, S. & CHKHEIDZE, N. 2014 Extremely efficient Zevatron in rotating AGN magnetospheres. *Mon. Not. R. Astron. Soc.* **445**, 4155.

OSMANOV, Z., MAHAJAN, S., MACHABELI, S. & CHKHEIDZE, N. 2015 Millisecond newly born pulsars as efficient accelerators of electrons. *Nat. Sci. Rep.* **5**, 14443–14454.

OSMANOV, Z., SHAPAKIDZE, D. & MACHABELI, G. 2009 Dynamical feedback of the curvature drift instability on its saturation process. *Astron. Astrophys.* **503**, 19–24.

PELLETIER, G. 1982 Generation of a high-energy electron tail by strong Langmuir turbulence in a plasma. *Phys. Rev. Lett.* **49**, 782–785.

ROGAVA, A. D., DALAKISHVILI, G. & OSMANOV, Z. N. 2003 Centrifugally driven relativistic dynamics on curved trajectories. *Gen. Relativity Gravitation* **35**, 1133–1152.

RUDERMAN, M. A. & SUTHERLAND, P. G. 1975 Theory of pulsars – polar caps, sparks, and coherent microwave radiation. *Astrophys. J.* **196**, 51–72.

SHKLOVSKY, I. S. 1953 O svechenii Krabovidnoi tumannosti. *Dokl. Akad. Nauk* **90**, 983–994; (in Russian).

STURROCK, P. A. 1971 A model of pulsars. *Astrophys. J.* **164**, 529–556.

TADEMARU, E. 1973 On the energy spectrum of relativistic electrons in the Crab nebula. *Astrophys. J.* **183**, 625–635.

THORNE, K., PRICE, R. & MACDONALD, D. A. 1986 *Black Holes: the Membrane Paradigm*. Yale University Press.

VASHAKIDZE, M. A. 1954 O stepeni polarizacii blizkix vnegalakticheskix tumannostei I Krabovidnoi tumannosti. *Astr. Circ.* **149**, 11–14; (in Russian).

VEDENOV, A. A. & RUDAKOV, L. I. 1964 Interaction of waves in continuous media. *Dokl. Akad. Nauk SSSR* **159**, 767–775.

WEEKES, T., CAWLEY, M. F., FEGAN, D. J. *et al.* 1989 Observation of TeV gamma rays from the Crab nebula using the atmospheric Cerenkov imaging technique. *Astrophys. J.* **342**, 379–395.

ZAKHAROV, V. E. 1972 Collapse of Langmuir wave. *Zh. Eksp. Teor. Fiz.* **35**, 908–919.

https://doi.org/10.1017/S0022377816000416 Published online by Cambridge University Press